Motion Control of an Exoskeleton Robot using Electromyogram Signals

Mohammad Habibur Rahman, Cristobal Ochoa-Luna, Maarouf Saad, and Philippe Archambault

***Abstract*—**We have developed a seven degrees of freedom exoskeleton robot (ETS-MARSE) for rehabilitation and assistance of upper limb movements in physically disabled individuals with impaired upper-limb function. Here we propose a new control strategy to maneuver the ETS-MARSE using skin surface electromyogram (EMG) signals, which are though to reflect the user's intention of motion. It is expected that the input of EMG signals to the robot controller will help maneuvering the robot in real time in assisting the subject's arm motion. A nonlinear sliding mode control technique was used for this purpose, where EMG signals were used as input information to the controller. To evaluate the performance of the proposed control approach experiments were carried out with the healthy individuals. Experimental results indicate that with the proposed control strategy, ETS-MARSE can be effectively maneuvered with the EMG signals.

***Keywords*—**Electromyogram signals, Exoskeleton Robot, Motion control, Sliding mode control.

I. Introduction

To rehabilitates individuals with impaired upper-limb function, extensive research has been carrying on in the field of assistive technology and rehabilitation robotics [1-4]. To contribute in this program we have developed an exoskeleton robot (ETS-MARSE) for rehabilitation and for assisting movements of the shoulder, elbow, forearm and wrist joints [4, 5]. Different control strategies were proposed and implemented in our previous research to maneuver the ETS-MARSE in providing passive rehabilitation therapy [6-8]. In the "passive movement" approach, it is assumed that a subject is completely unable to move his arm and therefore the robot's task is to perform passive movement exercises (requiring no user effort) such as elbow flexion/extension, forearm pronation/supination etc. This type of therapy is mainly to increase joint range of motion. Following passive therapy, the next therapeutic mode which contributes to the restoration of upper extremity function is known as active rehabilitation therapy. In this approach subjects actively participate in performing the exercises such as a reaching movement exercise, with the robot providing support against gravity and assisting with movement if needed [9]. As a first step to provide such active therapy, we developed a control strategy based on the subject's surface EMG signals, which reflect the intention of movement. The primary objective of this research was to control an arm exoskeleton robot with the user's surface EMG signals.

Using EMG signals to control exoskeleton robots or, robotic prostheses has gained a lot of attention since the last decade [10-14]. Indeed, different types of EMG based control approaches are found in the literature. Kiguchi et al. [10] proposed a fuzzy-neuro control method to control a mobile exoskeleton robot. Khokhar et al. [14] used pattern recognition method for the control of a wrist exoskeleton. Liu et al in [15] proposed an adaptive EMG based robot control system via use of adaptive neuro-fuzzy inference system to manipulate an industrial robot. Shenoy et al. [16] used a support vector machine (SVM) classifier technique to control a robotic arm. All these methods are computationally expensive and are not robust to deal with the nonlinearity of EMG signals. In this research we proposed a new EMG based control strategy using sliding mode control with exponential reaching law (*SMERL*) [17, 18] to drive the ETS-MARSE.

Although the input to the controller is the user's skin surface EMG signals, this EMG signals are transformed into a position command. Therefore, the guiding principle of the ETS-MARSE is a position controller based on the EMG signals. Details of this control strategy are presented in section III, following a brief description of the ETS-MARSE (Section II). Experiments were carried out with healthy male subjects to control the ETS-MARSE with the EMG signals (Section IV). Finally, the paper ends with the conclusion in section V. It is anticipated that with the proposed control strategy, the ETS-MARSE can assist physically disabled individuals by providing them with arm motion.

II. Exoskeleton Robot, ETS-MARSE

The ETS-MARSE, as shown in Fig. 1, is a 7 degrees-of-freedom exoskeleton robot designed to be worn on the lateral side of upper extremity in order to provide naturalistic movements of the shoulder (i.e., vertical and horizontal flexion/extension, and internal/external rotation), elbow (i.e.,

M.H. Rahman is (Postdoctoral Fellow) with the School of Physical & Occupational Therapy, McGill University and (Research Assistant) Electrical Department, École de Technologie Superieure, Montreal, Canada (email: mhrahman@ieee.org).

M. Saad is with the Electrical Engineering Dept., École de Technologie Superieure, Montreal, Canada (email: maarouf.saad@etsmtl.ca).

C. Ochoa-Luna is (PhD candidate) with the Electrical Engineering Department, École de Technologie Superieure, Montreal, Canada (email: cristobal.ochoa-luna.1@ens.etsmtl.ca).

P. S. Archambault is with the School of Physical & Occupational Therapy, McGill University, Canada (email: philippe.archambault@mcgill.ca).

ISBN: 978-1-61804-242-2

flexion/extension), forearm (i.e., pronation/supination), and wrist joint (i.e., radial/ulnar deviation, and flexion/extension). Provision included in the design to adjust the link-lengths to accommodate a wide range of individuals. Brushless DC motors are used to actuate the ETS-MARSE. The individual joint's workspace of the ETS-MARSE is illustrated in Fig. 2.

Fig. 1 Exoskeleton Robot, ETS-MARSE

III. EMG Signals Processing

The central nervous system sends motor command to each muscle via motor neurons. These signals activate the skeletal muscles (i.e., contractions and tensions), and thus produce necessary joint torques for posture control and voluntary movements. Surface EMG signals are used to measure those motor commands to be sent to the muscles.

These EMG signals are highly nonlinear in nature. For instance, to perform the same upper-limb movements, EMG activity may vary from subject to subject. Even in the case where a same subject performs the same upper limb motion, EMG can vary depending on the subject's physiological condition such as fatigue, stress, placement of electrodes etc. These signals consist of a wide range of frequencies and it is often difficult to reduce noise by filtering. Therefore, raw EMG signals cannot be directly used to provide meaningful information to the controller. So, features have to be extracted from the noisy raw EMG signals. There are various features extraction methods. Some commonly used methods are: waveform length, mean absolute value, root mean square (RMS), average or full rectified value, zero crossing, slope sign changes, etc [19].

For this study RMS value is chosen to process raw EMG signals (±5mV). Note that, the RMS value is a measure of power of the signal and it is widely used in most applications.

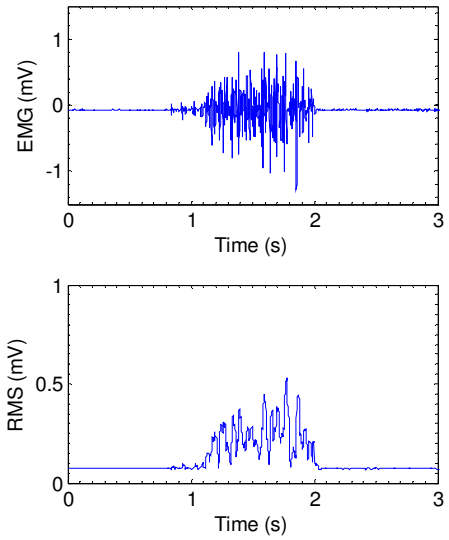

Fig. 3 Example of raw EMG signals and RMS value

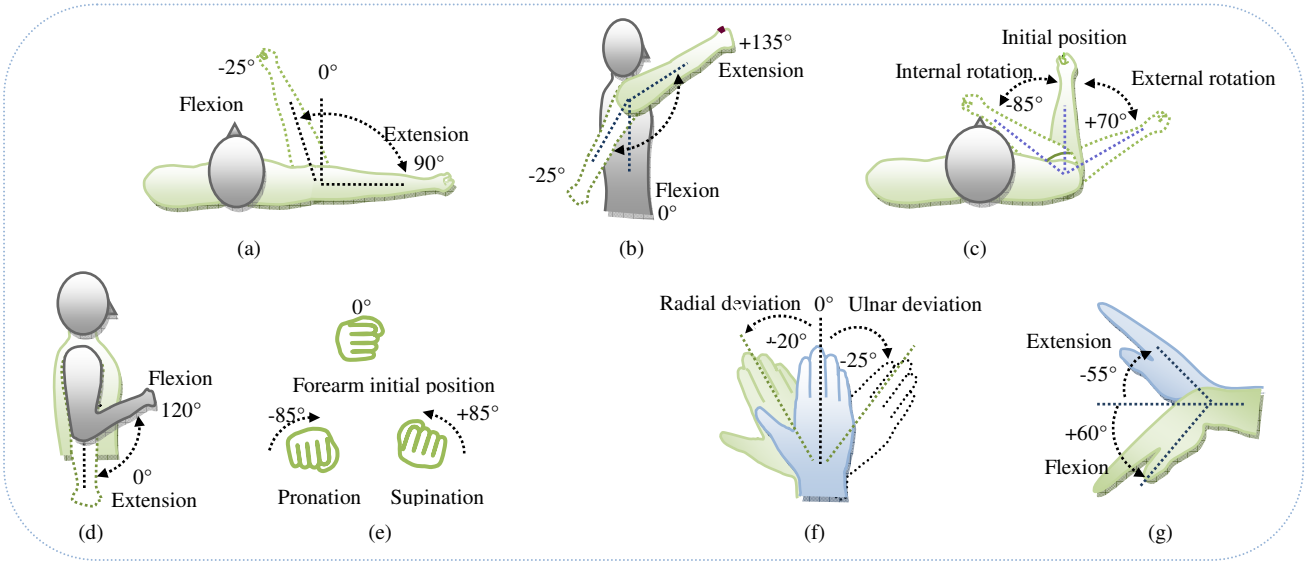

Fig. 2 Workspace of ETS-MARSE. (a) Joint-1: shoulder joint horizontal flexion-extension; (b) Joint-2: shoulder joint vertical flexion-extension; (c) Joint-3: shoulder joint internal-external rotation; (d) Joint-4: elbow flexion-extension; (e) Joint-5: forearm pronation-supination; (f) Joint-6: wrist joint radial-ulnar deviation; (g) Joint-7: wrist joint flexion-extension.

ISBN: 978-1-61804-242-2

The equation of RMS value is written as:

$$RMS = \sqrt{\frac{1}{N}\sum_{i=1}^{N} v_i^2} \quad (1)$$

where v_i is the voltage value at the i^{th} sampling and N is the number of sample in a segment. The number of samples is set to be 50 and the sampling time is 0.5msec.

An example of the RMS value of raw EMG signals recorded from elbow muscles (biceps brachii) is depicted in Fig. 3.

IV. Control Scheme

A. Muscle Modeling

Joint movements are controlled by the actions of agonist and antagonist muscles (such as biceps brachii for elbow flexion, triceps brachii for elbow extension motion etc.). For single joint movements, multiple agonists and antagonists muscles may be involved (e.g., shoulder joint vertical flexion is controlled by the posterior part of deltoid, teres major, and latissimus dorsi muscles) [20]. Some muscles are responsible for multiple joint movements (e.g., posterior part of deltoid is responsible for external rotation, horizontal extension, and vertical extension motion of shoulder joint). In this study we have studied the upper-limb muscles to find single dominating muscle responsible for a specific joint movement. The study was experimentally validated by analyzing EMG activity of healthy individuals' muscles. Table 1 gives the antagonist and agonist muscles used to develop the proposed EMG based control approach.

B. Control Strategy

It is the skeletal muscles' forces which produce joint torques for the joint movements. A force/torque applied at the wrist joint of upper-limb (or at the end-effector of ETS-MARSE) can produce the same joint torques, and may results the same joint motions. For instance, as shown in Fig. 4a, a force applied along Z axis (i.e., F_z) or a torque applied around Y axis (i.e., T_y) can produce the same torque as produced by the elbow muscles force (F_m, Fig. 4b) at the elbow joint. Similarly

Table 1. Agonist and antagonist muscles of upper-limb (shoulder elbow and forearm [20])

Upper-limb motion	Agonist/Antagonist Muscles
Shoulder joint vertical flexion	Deltoid anterior part
Shoulder joint vertical extension	Teres major
Shoulder joint horizontal flexion	Pectoralis major calvicular part
Shoulder joint horizontal extension	Deltoid posterior part
Shoulder joint internal rotation	Latissimus Dorsi
Shoulder joint external rotation	Supraspinatus
Elbow flexion	Biceps brachii
Elbow extension	Triceps brachii
Forearm pronation	Pronator teres
Forearm supination	Supinator

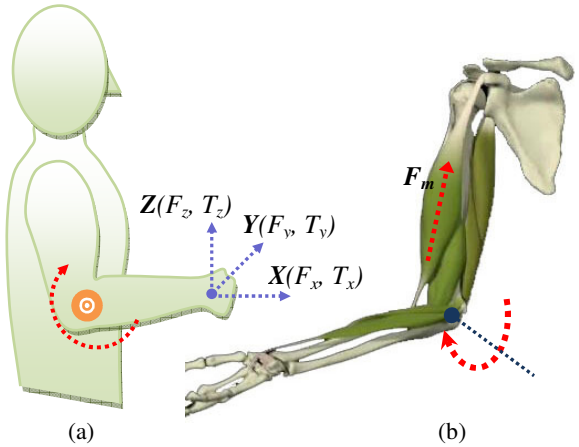

Fig. 4 Elbow joint flexion/extension mechanism. (a) Virtual force acting at the end-effector (wrist-joint), producing joint torques, (b) Elbow muscles producing equivalent elbow joint torques causing flexion/ extension motion.

a torque applied around X axis (T_x) will produce the same forearm motion as produced by the actions of pronator teres and supinator muscles. Therefore, in this case, the surface EMG signals, which are a measure of muscle activity, can be co-related to a virtual force/torque (F_v) acting at the wrist joint of a subject. Let's assume that EMG signals recorded from the agonist and antagonist muscles (EMG_i) for individual joint movements are proportional to the virtual force/torque vectors ($F_v \in \mathbb{R}^{6\times1}$). The relation can be expressed as:

$$F_v = \Delta C_i \times EMG_i \quad (2)$$

where ΔC_i = proportional constant for individual muscles.

Therefore, the virtual force/torque vector that represents the activity of agonist and antagonist muscles of elbow would be $F_{v\_el} = [0 \quad 0 \quad F_z \quad 0 \quad T_y \quad 0]^T$

where $F_z = \Delta C_{f_z i} \times EMG_i$, and $T_y = \Delta C_{T_y i} \times EMG_i$.

Similarly, for shoulder joint internal/external rotation due to the activity of agonist and antagonist muscles of shoulder, it would be $F_{v\_sR} = [0 \quad F_y \quad 0 \quad 0 \quad 0 \quad T_z]^T$.

Consider a 6-axis virtual force/torque sensor (representing EMG activity of muscles) instrumented at the end-effector of the ETS-MARSE (Fig. 1). The simplified control architecture of the ETS-MARSE control system is depicted in Fig. 5. The principle of EMG based control approach (or active exercise) is that the subjects initiate the movement to complete a specified task.

As seen from the schematic (Fig. 5), control is carried out based on the skin surface EMG signals of subjects. The instantaneous EMG signals of muscles (i.e., subject's initiation of movement) and the previous joint angles of the ETS-MARSE are used to compute the desired position command (joint angles) of the robot to follow, which can be expressed as:

ISBN: 978-1-61804-242-2

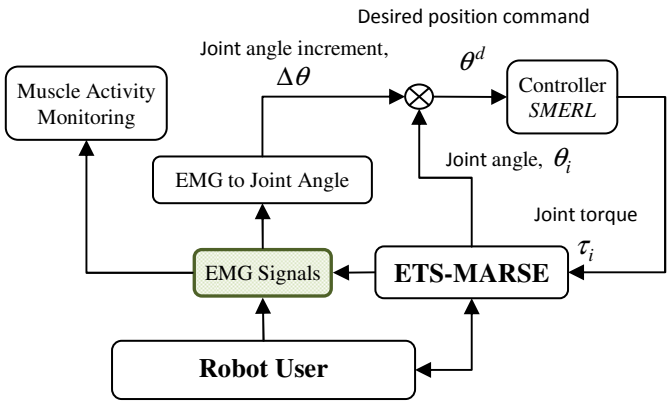

Fig. 5 Schematic diagram of EMG based control system

$$\theta^d = \theta_{old} + \Delta\theta\left(\tau_v(EMG_i)\right) \tag{3}$$

where $\theta^d \in \mathbb{R}^{7\times1}$ is the desired joint angles vector, $\theta_{old} \in \mathbb{R}^{7\times1}$ is the previous joint angles vector, and $\Delta\theta \in \mathbb{R}^{7\times1}$ is the vector of infinitesimal changes of joints' angles corresponding to the instantaneous change of EMG signals, and $\tau_v \in \mathbb{R}^{7\times1}$ is the virtual torques vector. Note that, the virtual force/torques $F_v \in \mathbb{R}^{6\times1}$ as applied at the end-effector corresponding to the instantaneous change of EMG signals produce joints' torques ($\tau_v \in \mathbb{R}^{7\times1}$) which can be expressed by the following relation.

$$\tau_v = J^T(\theta)F_v \tag{4}$$

where $J(\theta) \in \mathbb{R}^{6\times n}$ is the Jacobian matrix of ETS-MARSE (n=7), and $\theta \in \mathbb{R}^{7\times1}$ is the joint angle vector.

The change of joints' angle corresponding to the infinitesimal changes of $F_v \in \mathbb{R}^{6\times1}$ is thus assumed to be proportional to the corresponding joints' torques $\Delta\tau_v \in \mathbb{R}^{7\times1}$, that is-

$$\Delta\tau_v = K_{pG}\Delta\theta \tag{5}$$

where $K_{pG} \in \mathbb{R}^{7\times7}$ is the (diagonal) proportional gain matrix that transforms infinitesimal changes of joints' torques $(\Delta\tau_v)$ to the corresponding joint angles $(\Delta\theta)$. A detail of this transformation can be found in [21].

So, the sliding mode exponential reaching law *(SMERL),* as depicted in the schematic (Fig. 5), works mainly on the position regulation of the ETS-MARSE. In the next sub-section, the theoretical structure of the sliding mode control technique with exponential reaching law (ERL) is presented for the dynamic trajectory tracking of the ETS-MARSE.

C. Sliding mode control with ERL

The dynamic behaviour of the ETS-MARSE can be expressed by the well-known rigid body dynamic equation as:

$$M(\theta)\ddot{\theta} + V(\theta,\dot{\theta}) + G(\theta) + F(\theta,\dot{\theta}) = \tau \tag{6}$$

where $M(\theta) \in \mathbb{R}^{7\times7}$ is the inertia matrix, $V(\theta,\dot{\theta}) \in \mathbb{R}^{7\times1}$ is the coriolis/centrifugal vector, $G(\theta) \in \mathbb{R}^{7\times1}$ is the gravity vector, and $F(\theta,\dot{\theta}) \in \mathbb{R}^{7\times1}$ is the friction vector. Note that the friction vector is modeled as a nonlinear coulomb friction, and can be expressed as:

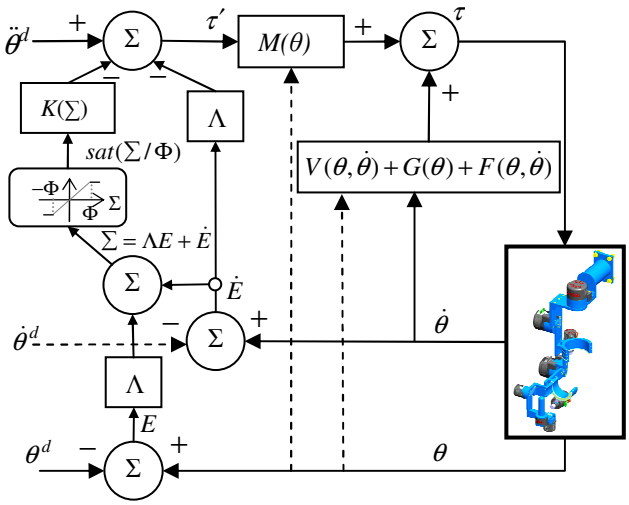

Fig. 6. Schematic diagram of sliding mode exponential reaching law in combination with *sat* function

$$\tau_{friction} = F\left(\theta,\dot{\theta}\right) = c\,sgn\left(\dot{\theta}\right) \tag{7}$$

where c is the coulomb-friction constant. Equation (6) can be written as:

$$\ddot{\theta} = -M^{-1}(\theta)\left[V\left(\theta,\dot{\theta}\right) + G\left(\theta\right) + F\left(\theta,\dot{\theta}\right)\right] + M^{-1}\left(\theta\right)\tau \tag{8}$$

$M^{-1}(\theta)$ always exists since $M(\theta)$ is symmetrical and positive definite. The general layout of the sliding mode control technique is depicted in Fig. 6. The initial step in the sliding mode control is to choose the sliding (or switching) surface S in terms of the tracking error. Let the tracking error for each joint be defined as:

$$e_i = \theta_i - \theta_i^d \quad \cdots \quad (i = 1,\cdots,m) \tag{9}$$

and the sliding surface as:

$$S_i = \lambda_i e_i + \dot{e}_i \quad \cdots \quad (i = 1,\cdots,m) \tag{10}$$

where θ_i^d is the desired trajectory for joint i and S_i is the sliding surface of each DoF.

Let $\Sigma = \begin{bmatrix} S_1 & S_2 & \cdots & S_m \end{bmatrix}^T$ be the sliding surface for the ETS-MARSE. Therefore, we have:

$$\Sigma = \begin{bmatrix} \lambda_1 e_1 + \dot{e}_1 \\ \vdots \\ \lambda_m e_m + \dot{e}_m \end{bmatrix} \tag{11}$$

Equation (11) is a first order differential equation, which implies that if the sliding surface is reached, the tracking error will converge to zero as long as the error vector stays on the surface.

ISBN: 978-1-61804-242-2

Considering the following Lyapunov function candidate:

$$V = \frac{1}{2}\Sigma^T\Sigma \tag{12}$$

which is continuous and nonnegative, the derivative of V yields:

$$\dot{V} = \Sigma^T\dot{\Sigma} \tag{13}$$

By choosing $\dot{\Sigma}$ as given in equation (14) relation (13) is ensured to be decreasing.

$$\dot{\Sigma} = -K\,sign(\Sigma)\ ,\ \forall t, K>0 \ \Rightarrow\ \dot{V}<0 \tag{14}$$

where

$$sign(\Sigma) = \begin{cases} 1\ for\ \Sigma>0 \\ 0\ for\ \Sigma=0 \\ -1\ for\ \Sigma<0 \end{cases} \tag{15}$$

Expression (14) is known as the reaching law. It is to be noted that the discontinuous term $K\,sign(\Sigma)$ in (14) often leads to a high control activity, known as chattering. One of the most known approaches found in the literature is to smoothen the discontinuous term in the control input with the continuous term $K\,sat(\Sigma/\phi)$ [22].

where

$$sat(\Sigma/\phi) = \begin{cases} \Sigma/\phi & for \quad \left|\Sigma/\phi\right| \le 1 \\ 0 & for \quad \Sigma/\phi = 0 \\ sign(\Sigma/\phi) & for \quad \left|\Sigma/\phi\right| > 1 \end{cases} \tag{16}$$

Using equation (16), the reaching law therefore becomes:

$$\dot{\Sigma} = -K\,sat(\Sigma/\phi)\ ,\ \forall t, K>0 \tag{17}$$

By performing this substitution, the convergence of the system stays within a boundary layer neighborhood (defined by Φ) of the switching surface. Therefore, with this approach, the chattering level is controlled in exchange of tracking performance. We have already demonstrated in our previous research [17] that the reaching law which combines ERL [18] with *sat* function [22] significantly reduce chattering and improve tracking. The ERL can be expressed as:

$$\dot{\Sigma} = -K(\Sigma)\,sign(\Sigma)\ ,\ \forall t, K>0 \tag{18}$$

where

$$K(\Sigma) = diag\left(\frac{k_i}{N_i(S_i)}\right) \quad \ldots\ (i=1,\ldots,m), \text{ and} \tag{19}$$

$$N_i(S_i) = \delta_{0i} + (1-\delta_{0i})e^{-\alpha_i|S_i|^{P_i}} \tag{20}$$

where $0<\delta_{0i}\le 1;\ \alpha_i>0,$ and, $P_i>0.$

The values of δ_{0i}, α_i, and P_i can be fixed as proposed in [18]. The new reaching law that combines the *sat* function and the concept of ERL can be written as follows:

$$\dot{\Sigma} = -K(\Sigma)\,sat(\Sigma/\phi)\ ,\ \forall t, K>0 \tag{21}$$

Therefore and considering

$$\ddot{\theta}^d = [\ddot{\theta}_1^d \quad \ddot{\theta}_2^d \quad \cdots \quad \ddot{\theta}_m^d]^T,$$

$$\dot{E} = [\dot{e}_1 \quad \dot{e}_2 \quad \cdots \quad \dot{e}_m]^T, \text{ and } \Lambda = diag[\lambda_i \quad \cdots \quad \lambda_m]$$

$$\Sigma = \Lambda E + \dot{E} \quad \Rightarrow \quad \dot{\Sigma} = \Lambda\dot{E} + \ddot{E} \tag{22}$$

where, $\ddot{E} = \ddot{\theta} - \ddot{\theta}^d$. Thus, relation (22) can be written as:

$$\dot{\Sigma} = \Lambda\dot{E} + \ddot{\theta} - \ddot{\theta}^d \tag{23}$$

Substituting the value of $\ddot{\theta}$ from equation (8) in equation (23) we obtain:

$$\begin{aligned}\dot{\Sigma} &= \Lambda\dot{E} - \ddot{\theta}^d + M^{-1}(\theta)\tau \\ &\quad -M^{-1}(\theta)\left[V(\theta,\dot{\theta}) + G(\theta) + F(\theta,\dot{\theta})\right]\end{aligned} \tag{24}$$

Replacing $\dot{\Sigma}$ by its value given in equation (21):

$$\begin{aligned}&-K(\Sigma)\,sat(\Sigma/\phi) = \Lambda\dot{E} - \ddot{\theta}^d \\ &-M^{-1}(\theta)\left[V(\theta,\dot{\theta}) + G(\theta) + F(\theta,\dot{\theta}) - \tau\right]\end{aligned} \tag{25}$$

The torque τ can be isolated and thus yields:

$$\begin{aligned}\tau &= -M(\theta)\left(\Lambda\dot{E} - \ddot{\theta}^d + K(\Sigma)\,sat(\Sigma/\phi)\right) \\ &\quad +\left[V(\theta,\dot{\theta}) + G(\theta) + F(\theta,\dot{\theta})\right]\end{aligned} \tag{26}$$

where K and Λ are diagonal positive definite matrices. Therefore, the control law given in equation (26) ensures that the control system is stable. A detailed explanation of the stability analysis is given in [17].

V. Experiments and Results

Experimental setup of the developed ETS-MARSE system is depicted in Fig. 7. It consists of a CPU processor (NI PXI-8108) with a reconfigurable FPGA (field-programmable gate array), seven motor drivers, a custom designed main board,

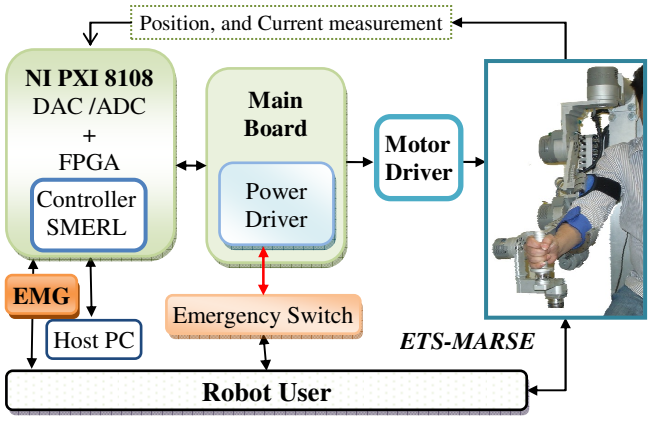

Fig. 7. Experimental setup.

Fig. 8 Electrode placement for elbow joint flexion/extension, forearm pronation supination and shoulder joint vertical flexion/extension motion

the triceps is shown in Fig. 9b. The elbow joint angles of ETS-MARSE corresponding to the biceps and triceps actions are shown in the Fig. 9c. It can be seen from the Fig. 9c, that when triceps is activating it produces extension motion of ETS-MARSE and when biceps is activating it produces flexion motion of ETS-MARSE. The trail was performed in different velocities for 30 sec. In all cases the developed EMG based control approach was able to maneuver the ETS-MARSE effectively and smoothly in providing flexion/extension motion of elbow joint using the EMG signals of muscles. Therefore, the control approach as proposed in this research can be effectively used in providing active rehabilitation exercises.

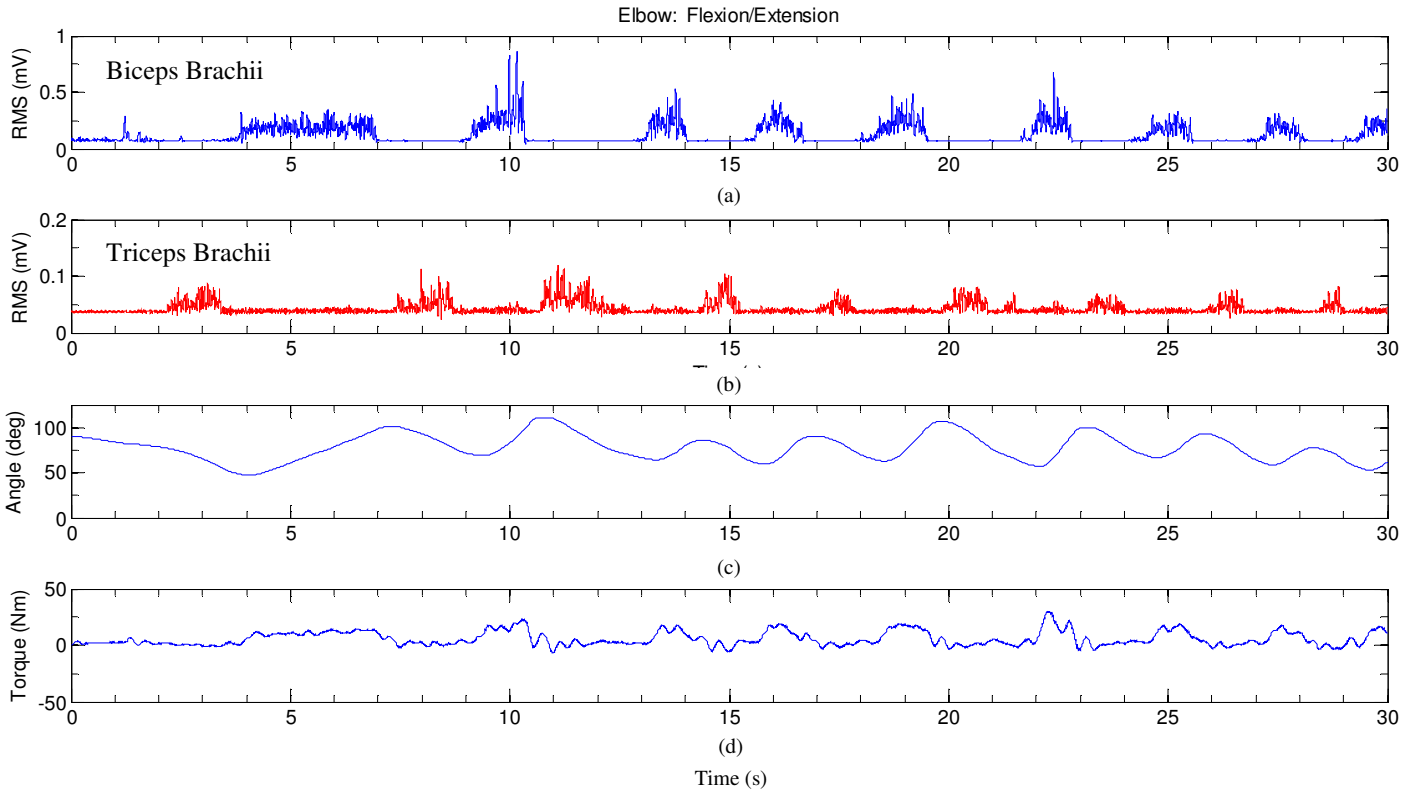

Fig. 9 Elbow joint flexion/extension motion

and a host PC. The main board as shown in Figure 7 acts as a motherboard, and is powered by an AC 120V (60Hz) power supply. The motherboard routes various analog and digital signals from/to the NI-PXI to/from the ETS-MARSE system. The control algorithm is executed in the NI-PXI.

The EMG electrodes (Delsys) placement on upper-limb muscles are depicted in Fig. 8. In this study, elbow muscles (e.g., biceps and triceps) of the subjects are monitored and used as input information to control of the ETS-MARSE. The experiment was conducted with subjects in a seated position with elbow joint angle at 90°. In experiments, the performance of the proposed EMG based control approach for motion control of the ETS-MARSE was evaluated. The experimental result for elbow joint flexion/extension movement is depicted in Fig. 9. The top most plots show the RMS values of EMG signals recorded from the biceps brachii muscle and that for

VI. Conclusion

A new EMG based control strategy as proposed in this research was experimentally evaluated for the motion control of ETS-MARSE. A brief description of the ETS-MARSE was presented. A detail of the proposed control strategy was also presented. From the experimental results, it is evident that with the developed control approach the ETS-MARSE will be able to provide active assistance in arm movements. Future works will include developing a hybrid controller with the fusion of the force sensor based controller and the EMG based controller.

Acknowledgment

The first author gratefully acknowledges the support provided for this research through a FRQNT-B3 (Fonds de

recherche du Québec – Nature et technologies) scholarship. The authors also acknowledge the support provided for this research by the INTER (le Groupe Ingénierie des technologies interactives en réadaptation) research group.

REFERENCE

[1] K. Kiguchi, M. H. Rahman, and T. Yamaguchi, "Adaptation strategy for the 3DOF exoskeleton for upper-limb motion assist," in *2005 IEEE International Conference on Robotics and Automation, April 18, 2005 - April 22, 2005*, Barcelona, Spain, 2005, pp. 2296-2301.

[2] K. Nagai, I. Nakanishi, H. Hanafusa, S. Kawamura, M. Makikawa, and N. Tejima, "Development of an 8 DOF robotic orthosis for assisting human upper limb motion," presented at the 1998 IEEE International Conference on Robotics and Automation, Leuven, Belgium, 1998.

[3] T. Nef, M. Mihelj, and R. Riener, "ARMin: a robot for patient-cooperative arm therapy," *Medical & Biological Engineering & Computing,* vol. 45, pp. 887-900, Sep 2007.

[4] M. H. Rahman, M. J. Rahman, O. L. Cristobal, M. Saad, J. P. Kenne, and P. S. Archambault, "Development of a Whole arm Wearable Robotic Exoskeleton for Rehabilitation and to Assist Upper Limb Movements," *Robotica,* DOI: http://dx.doi.org/10.1017/S0263574714000034, Published online: 28 January 2014, pp. 1-21, 2014.

[5] M. H. Rahman, M. Saad, J. P. Kenne, and P. S. Archambault, "Modeling and Development of an Exoskeleton Robot for Rehabilitation of Wrist Movements," in *2010 IEEE/ASME International Conference on Advanced Intelligent Mechatronics (AIM 2010), 6-9 July 2010*, Montreal, Canada, 2010, pp. 25-30.

[6] M. H. Rahman, P. S. Archambault, M. Saad, O. L. Cristobal, and S. B. Ferrer, "Robot Aided Passive Rehabilitation using Nonlinear Control Techniques," presented at the Asian Control Conference (ASCC 2013), Istanbul, Turkey, 2013.

[7] M. H. Rahman, O. L. Cristobal, M. Saad, J. P. Kenne, and P. S. Archambault, "Cartesian Trajectory Tracking of an Upper Limb Exoskeleton Robot " in *IECON 2012*, Montreal, 2012.

[8] M. H. Rahman, M. Saad, J. P. Kenne, and P.S. Archambault, "Robot assisted rehabilitation for elbow and forearm movements," *Int. J. Biomechatronics and Biomedical Robotics,* vol. 1, pp. 206-218, 2011.

[9] M. H. Rahman, M. J. Rahman, M. Saad, O. L. Cristobal, and P. S. Archambault, "Control of an Upper Extremity Exoskeleton Robot to Provide Active Assistive Therapy," *International Conference on Modelling, Identification & Control (ICMIC)* pp. 105-110, 31stAug.-2ndSept. 2013 2013.

[10] K. Kiguchi, M. H. Rahman, and M. Sasaki, "Neuro-fuzzy based motion control of a robotic exoskeleton: considering end-effector force vectors," in *Proceedings. 2006 Conference on International Robotics and Automation*, Orlando, FL, USA, 2006, pp. 3146-8.

[11] S. Komada, Y. Hashimoto, N. Okuyama, T. Hisada, and J. Hirai, "Development of a Biofeedback Therapeutic-Exercise-Supporting Manipulator," *IEEE Transactions on Industrial Electronics,* vol. 56, pp. 3914-3920, Oct 2009.

[12] L. Lucas, M. DiCicco, and Y. Matsuoka, "An EMG-Controlled Hand Exoskeleton for Natural Pinching," *Journal of Robotics and Mechatronics,* vol. 16, pp. 482-488, 2004.

[13] J. Rosen, M. Brand, M. B. Fuchs, and M. Arcan, "A myosignal-based powered exoskeleton system," *IEEE Transactions on Systems Man and Cybernetics Part a-Systems and Humans,* vol. 31, pp. 210-222, May 2001.

[14] Z. O. Khokhar, Z. G. Xiao, and C. Menon, "Surface EMG pattern recognition for real-time control of a wrist exoskeleton," *Biomed Eng Online,* vol. 9, p. 41, 2010.

[15] H. J. Liu and K. Y. Young, "An Adaptive Upper-Arm EMG-Based Robot Control System," *International Journal of Fuzzy Systems,* vol. 12, pp. 181-189, Sep 2010.

[16] P. Shenoy, K. J. Miller, B. Crawford, and R. P. N. Rao, "Online electromyographic control of a robotic prosthesis," *Ieee Transactions on Biomedical Engineering,* vol. 55, pp. 1128-1135, Mar 2008.

[17] M. H. Rahman, T. K. Ouimet, M. Saad, J. P. Kenne, and P. S. Archambault, "Control of an Exoskeleton Robot Arm with Sliding Mode Exponential Reaching Law," *International Journal of Control, Automation and Systems,* vol. 11, no.1, pp.92-104, 2013.

[18] C. J. Fallaha, M. Saad, H. Y. Kanaan, and K. Al-Haddad, "Sliding-Mode Robot Control With Exponential Reaching Law," *IEEE Transactions on Industrial Electronics,* vol. 58, pp. 600-610, 2011.

[19] K. Kiguchi, M. H. Rahman, M. Sasaki, and K. Teramoto, "Development of a 3DOF mobile exoskeleton robot for human upper-limb motion assist," *Robotics and Autonomous Systems,* vol. 56, pp. 678-691, Aug 31 2008.

[20] H. Gray and C. D. Clemente, *Anatomy of the human body*, 30th American ed. Philadelphia: Lea & Febiger, 1985.

[21] M. H. Rahman, T. K. Ouimet, M. Saad, J. P. Kenne, and P. S. Archambault, "Development of a 4DoFs Exoskeleton Robot for Passive Arm Movement Assistance," *Int. J. Mechatronics and Automation,* vol. 2, no.1, pp. 34-50, 2012.

[22] H. Khalil, *Nonlinear systems*, 3rd ed. Upper Saddle River, N.J.: Prentice Hall, 2002.